Eur. Phys. J. B **11**, 609–614 (1999)

THE EUROPEAN PHYSICAL JOURNAL B

EDP Sciences

Morphology transition and slow dynamics in the collapse of amphiphilic monolayers at the air-water interface

E. Hatta[1,a], D. Suzuki[1], and J. Nagao[2]

[1] Nanoelectronics Laboratory, Graduate School of Engineering, Hokkaido University, Sapporo 060 - 0813, Japan
[2] Materials Division, Hokkaido National Industrial Research Institute, AIST, MITI, Sapporo 062 - 8517, Japan

Received 11 January 1999

Abstract. The morphology on collapsed monolayers at the air-water interface has been studied using phase contrast microscopy. It is found that the transition from randomly distributed to quasi-one dimensional crack pattern takes place, depending on the pH value of the subphase and the presence of specific divalent metal ions. In these macroscopic patterns, the former exhibits a surface roughening due to a monolayer buckling while the latter becomes more smooth and uniform. The occurrence of the former is instantaneous and the latter follows a slow dynamics, *i.e.*, the crack propagation in monolayers occurs with a delay for crack nucleation. Thus the change of pattern indicates the existence of a dynamic transition. The transition is discussed with the scenario of a crack instability in brittle materials. The changes of viscous nature and of ion binding, and the compression direction probably operate for the observed behavior effectively.

PACS. 68.18.+p Langmuir-Blodgett films – 46.50.+a Fracture mechanics, fatigue and cracks – 81.40.Np Fatigue, corrosion fatigue, embrittlement, cracking, fracture and failure

1 Introduction

A surprising wide variety of physical and chemical systems exhibit intriguing patterns and forms on their characteristic scales in equilibrium and nonequilibrium conditions [1,2]. Floating monolayers at the air-water interface display many modulated domain structures on macroscopic scales [3–5]. A lot of experimental and theoretical works have focused on their domain shapes and patterns [6]. It is the physics of these domain boundaries, dynamics and instabilities, which holds the key for understanding the principles of the formation of various shapes and patterns in these soft condensed matters. The interplay of long-range electrostatic dipolar repulsion and line energy can result in interfacial instabilities [7].

Some effort, on the other hand, has also been devoted to a better understanding of crack pattern formation in soft matters such as polymer films [8], colloidal suspensions [9] and amphiphilic monolayers at the air-water interface [10]. A cracking phenomenon is one of the most significant nonequilibrium dissipative phenomena, where local disorder and non-linearity at a local scale strongly influence global behavior [11]. It involves a variety of processes occurring on a wide range of time and length scales. It is still, however, poorly understood. Amphiphilic monolayers at the air-water interface provide a quasi-two dimensional system with the degrees of orientational and conformational freedom of constituent molecules. Possibly, the existence of the internal degrees of freedom has a significant effect on the fragile nature of monolayers and facilitates the observations of different static patterns and dynamic behaviors in cracking. The stability and structure of amphiphilic monolayers at the air-water interface are strongly affected by the pH value of the subphase and the presence of divalent ions [12]. These factors are thus expected to affect the crack patterns and their dynamics decisively. Phase contrast microscopy allows the domain shapes and patterns of floating monolayers with no fluorescence to be determined by direct observation without adding probe materials [13] and opens up the possibility of following the dynamics of monolayers [10].

In this study we describe the macroscopic morphology and the dynamics of cracks in the collapse process of amphiphilic monolayers at the air-water interface. We demonstrate that they are strongly related and that a striking morphology transition occurs with a slow dynamics.

2 Experimental

Monolayers of stearic acid (C18, 99% pure, Sigma Chemicals) dissolved in *n*-hexane (99% pure, Kanto Chemicals) at a concentration of 0.5 mM were spread on a subphase (Millipore Mill-Q system filtered water, 18.0 MΩ-cm) containing 1.0 mM $CoCl_2$ (Rare Metallic, purity 99.999%) at 20.0 $\pm 0.2\,^{\circ}$C. The pH values of the subphase from 6.0 to 7.5 were adjusted with $NaHCO_3$. These materials were used without further purification.

[a] e-mail: hatta@nano.eng.hokudai.ac.jp

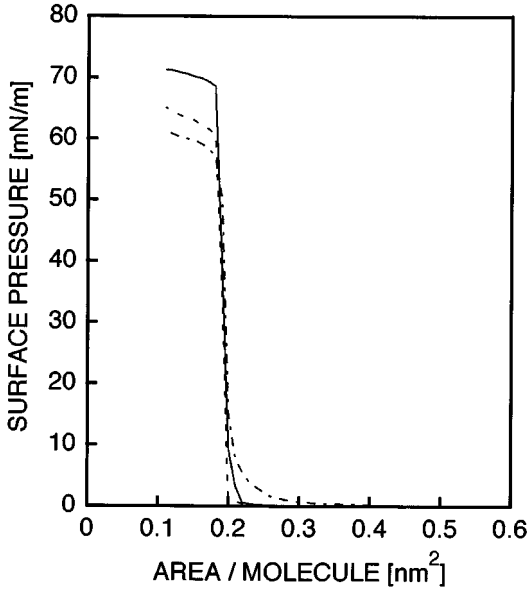

Fig. 1. Surface pressure as a function of area per molecule for stearic acid monolayers in the presence of 1.0 mM $CoCl_2$ and at pH 6.0 (solid curve), 7.0 (dashed curve) and 7.5 (dash-dotted curve), respectively.

Monolayers formed at the air-water interface were visualized with a phase contrast microscope (NIKON, OPTIPHOTO-2) equipped with a CCD camera followed by an image processor. The incident light was transmitted from the bottom of a glass trough equipped with the stage of the microscope. Monolayers were compressed at a speed of 1 cm/min by a barrier. The solid domain growth and subsequent crack propagation were recorded every 1/30 s by a video-recorder. Surface pressure (π) - area (A) isotherms were simultaneously measured.

3 Results and discussion

Figure 1 shows $\pi-A$ isotherms for stearic acid monolayers in the presence of 1.0 mM $CoCl_2$ and at the pH range of 6.0−7.5. The collapse pressure is seen to decrease monotonously with increasing pH values. This result demonstrates that the change of ionic conditions (*i.e.*, ion binding) strongly affects the mechanical stability in floating monolayers.

When monolayers are compressed above the collapse pressures, the irreversible monolayer fracture starts and numerous cracks occur. In Figure 2, typical crack patterns are shown for the same pH values as in Figure 1. Monolayers are compressed from left to right by a barrier in all images. In Figure 2a, cracks are observed to develop in various directions and to have non-uniform widths. As is evident from the intensity variation in numerous cracks, surface roughening appears clearly. Previous work suggests that the similar patterns are ridges coming out of the monolayer, *i.e.*, a localized monolayer buckling [14]. Figure 2c, on the other hand, exhibits a quite different crack pattern; these cracks become smooth and have a uniform width throughout just like the fracture in viscous glasses. Moreover, it is worth noting that the crack pattern becomes highly anisotropic. The intermediate pH pattern (Fig. 2b) shows the transient one between the above two, where the both characteristic features coexist.

A characteristic time scale is expected to be involved for the crack development. We examined images one by one to evaluate the time scale over which the cracks develop. Figures 3 shows the evolution of a crack in a solid domain at pH 6.0. The crack is seen to develop across the window instantaneously within 1/30 s. Surface roughening is clearly seen due to monolayer buckling. At pH 7.5, we find out that the crack development is dominated by a slow dynamics (Fig. 4). At the initial stage, the small, discrete cracks nucleate (Fig. 4b) and subsequently, the long smooth crack develops as joined initial discrete cracks together, and stops (Fig. 4c). Again the smooth crack develops after some intermission while the initial discrete cracks nucleate. Such a delayed fracture is not expected to be observable in three dimensions [15]. We define here the average crack velocity as the displacement of the crack tip appeared as a continuous crack divided by the total time taken for the initial crack nucleation and the subsequent smooth crack propagation. A typical crack velocity was $100 \sim 300\,\mu$m/s. The crack behavior at the intermediate pH value (Fig. 5) exhibits both the characteristic features seen in Figures 3 and 4. The crack development from bottom to top in the middle of the image is similar to the crack behavior in Figure 3. In this case, however, surface roughening does not appear instantaneously; the crack propagation becomes somewhat slow. We can therefore trace the intermediate processes during crack propagation with surface roughening. And the crack propagation from top to bottom in the right part of the figure has rather similar characteristics to the monolayer cracking in Figure 4. The crack velocity, however, becomes faster and we cannot follow the development (nucleation) of the initial cracks as seen in Figure 4. The change of the crack pattern in Figure 1 thus indicates the existence of a dynamic transition clearly.

The evolution strongly reminds us of a scenario of fracture in brittle materials [16]. No plastic deformation was indeed found during the present observations, suggesting brittle fracture in the floating monolayers. It was previously reported that a floating monolayer behaves as a typical fragile object [10]. The velocity of a crack in brittle materials can be considered as a control parameter which determines the crack dynamics [17]. Above a critical speed the crack develops an instability associated with a strong increase of the surface roughness; when the crack velocity is lower than the critical speed, surfaces produced by the crack are smooth. This is why surface roughening is considered to be an efficient mechanism which allows the crack to dissipate energy. In our study, it is perhaps the amphiphilic nature of such molecules with flexible, hydrocarbon chains and polar heads that facilitates the observation of surface roughening *via* monolayer buckling. At much higher speed than the critical speed the well-known phenomenon of crack branching appears [17]. In our case, the evolution of cracks exhibited no crack

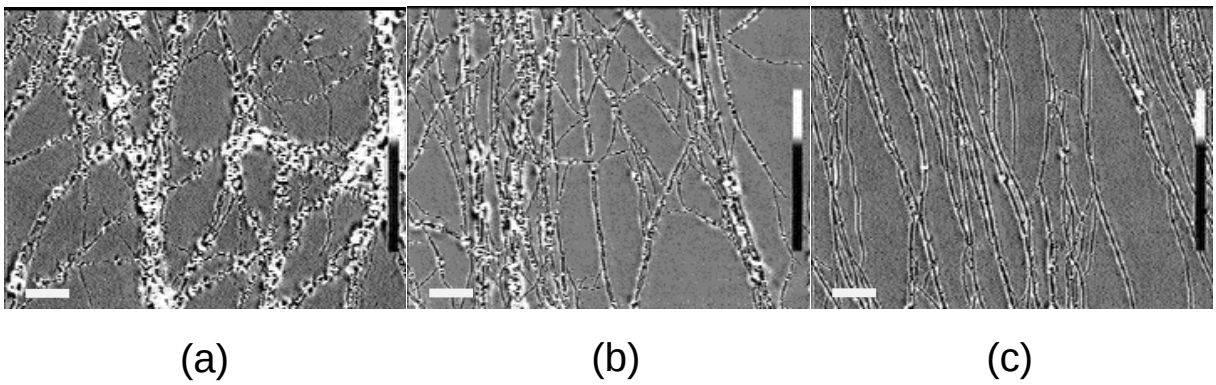

Fig. 2. Typical crack patterns for stearic acid monolayers in the presence of 1.0 mM $CoCl_2$ and at pH (a) 6.0, (b) 7.0, and (c) 7.5, respectively. A lot of crack lines are seen in each figure. Note that the fracture lines become more smooth and uniform and that the pattern changes to a more anisotropic one from (a) to (c). The bars represent 100 μm.

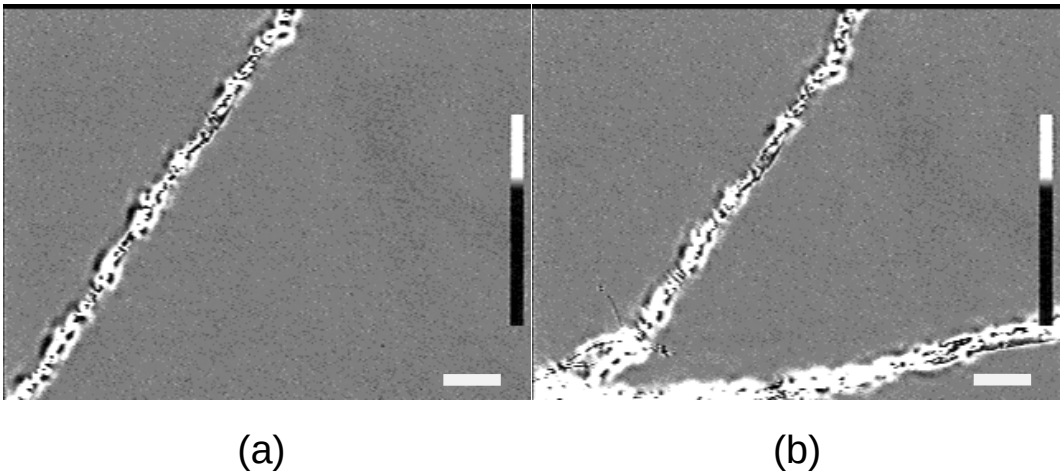

Fig. 3. Evolution of crack propagation in a stearic acid monolayer in the presence of 1.0 mM $CoCl_2$ and at pH 6.0. (b) is taken 0.03 s after (a). The crack line develops from left to right of the figure instantaneously. The bars represent 100 μm.

branching. Moreover the fact that the morphology transition from a pattern with surface roughening to one with more smooth surface was observed seems to support the idea that the change of this pattern has the nature of a dynamic transition across a critical speed, which we have not been able to determine exactly at present.

The floating monolayer on lateral compression beyond a certain pressure is in the high compressive stress state and stores strain energy. At pH 6.0, it is sufficient to understand that most of the stored strain energy is converted into the energy for breaking bonds between the molecules and subsequently that for the buckling of monolayer. On the other hand, at pH 7.5, the viscous nature of the solid domain perhaps leads to the slowing down of the crack propagation and hinders the monolayer buckling effectively. We emphasize features such as smoothness and uniformity which are common to the present static pattern (Fig. 2c) and that in a glass with a high viscosity. It should be remembered that the high viscous nature of solids generally tends to increase the time scale over which the related phenomena are observed. Indeed, from a molecular point of view, the existence of viscosity in the floating monolayer requires an additional loss of energy for constituent molecules to return to their original arrangements and orientations. The strain energy stored in the solid domain is then converted to the energy required to develop the cracks against the viscosity resistance. In this case, the strain energy stored and the energy for developing the cracks *via* the break of bonds can be sensitively balanced and thus the kinetic energy left to develop cracks further is small, which causes the slow dynamics of cracks, as characterized by the existence of an inherent relaxation time (typically, order of 10^{-1} s) for nucleating initial cracks.

The ionic condition determines the head group charge *via* proton dissociation and/or ion binding. In order to understand morphology transition and its dynamics, it is essential to take into account the effects of added divalent ions and the subphase pH and we carried out further experiments. We found the results for experiments

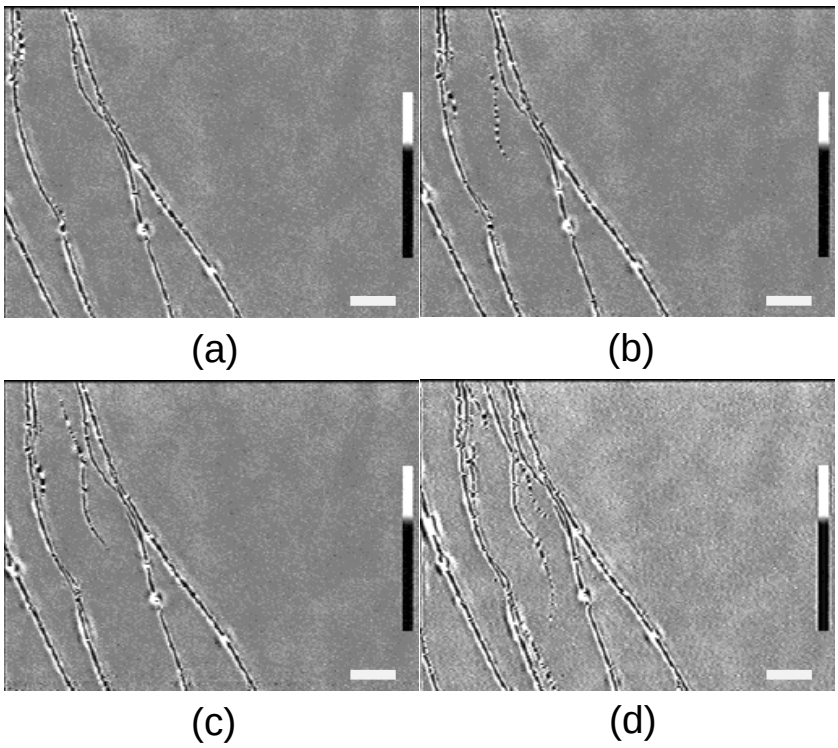

Fig. 4. Evolution of crack propagation in a stearic acid monolayer in the presence of 1.0 mM $CoCl_2$ and at pH 7.5. (b), (c), (d) are taken 0.60, 0.83 and 1.6 s after (a). First, the initial crack nucleation proceeds seen as small discrete, dark dots (b) and successively, the long crack line propagates (c). The crack develops by repeating this process. The bars represent 100 μm.

in the presence of other divalent ions such as Cd^{2+} and Mn^{2+} at the same pH range showed no significant morphology transition; they exhibited randomly distributed crack patterns only. Moreover, in the presence of Co^{2+} and at pH 7.8, the transition to the solid state on monolayer compression became largely gentle in the isotherm and exhibited no break corresponding to the onset of the monolayer collapse. In practice, the phase contrast microscope observation did not show an anisotropic but a random crack pattern. The cracking behavior observed in the presence of Co^{2+} and at pH 7.5 (Fig. 2c) thus appears to be unique. This suggests that at a rather narrow pH window anisotropic cracks are observed. While we cannot deduce the underlying structure of the monolayer on a molecular level from our macroscopic observations directly, we can say that the subphase pH and added specific ions (*i.e.*, Co^{2+}) combine to cause a striking morphology transition and a slow dynamics of the crack pattern.

We now consider an anisotropic nature of the crack pattern typically observed in monolayers at pH 7.5. Clearly, the revelation of such an anisotropy of cracks observed is a macroscopic manifestation of the nature of substances in which the cracks develop. An essential property of the cracks observed here is that the substance is composed not of simple rigid particles but of flexible molecules binded by divalent metal ions. The crack morphology and the kinetics are thus considered to depend strongly on the conditions of ion binding. The result of the experiment on the effect of the absence of divalent metal ions on the crack morphology is shown in Figure 6. This image is in marked contrast with those we presented in Figures 2–5. In this image, we find that a bulk phase [18] grows seen as numerous fine, dark spots throughout the area and definite crack lines are never seen. The images that have been shown so far allow one to conclude that the long crack propagation is certainly due to the existence of divalent metal ions in the subphase which leads to the anchoring (binding) between molecules. With this, the fact that the variations of macroscopic cracking patterns occur with changing the ionic conditions (Fig. 2), means that cracking behaviors are influenced by the conditions of ion binding significantly. In fact, it was reported that the composition ratio of salt and stearic acid in the barium stearate LB films varies with pH range 6.0−8.5 [19]. Moreover, we note that crack propagates roughly perpendicularly to the compression direction with increasing pH values. From the above considerations, the conditions of ion binding and the compression direction are believed to be two relevant parameters for causing the anisotropic crack pattern; however, further experiments are necessary to clarify the origin of anisotropy cracks.

4 Conclusions

We studied the patterns of cracks formed and their dynamics during the compression of amphiphilic monolayers at the air-water interface. The morphology transition from randomly distributed cracking pattern to highly

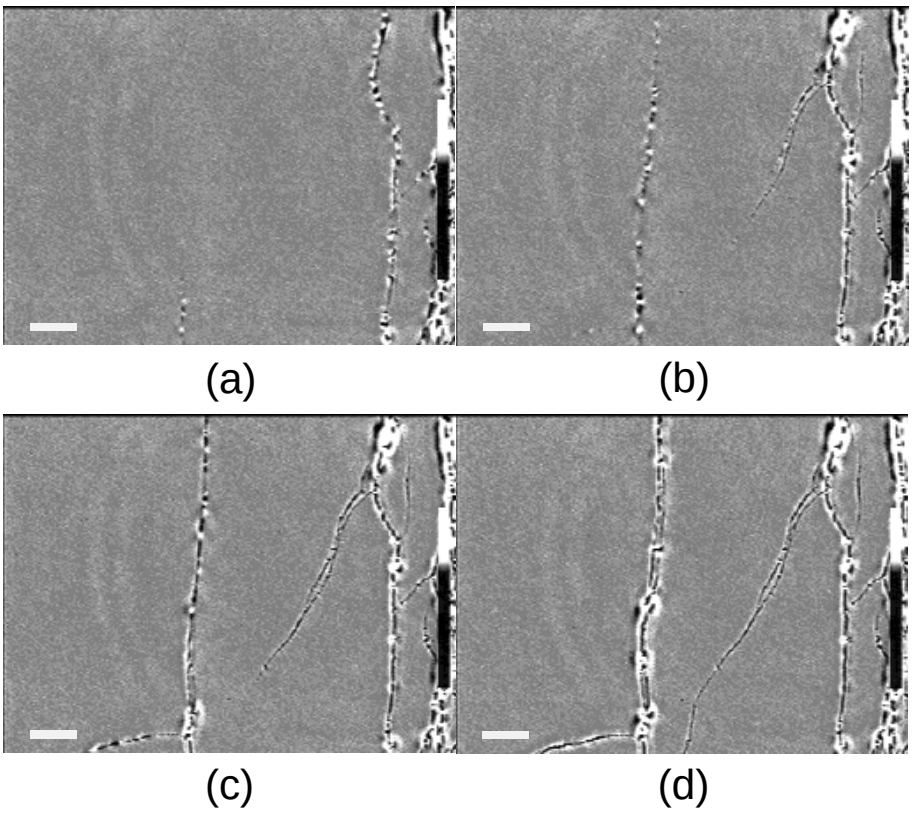

Fig. 5. Evolution of crack propagation in a stearic acid monolayer in the presence of 1.0 mM $CoCl_2$ and at pH 7.0. (b), (c), (d) are taken 0.03, 0.10 and 0.13 s after (a). The crack developments from bottom to top and from top to bottom of the figure exhibit the similar characteristics to those in Figures 3 and 4, respectively. The bars represent 100 μm.

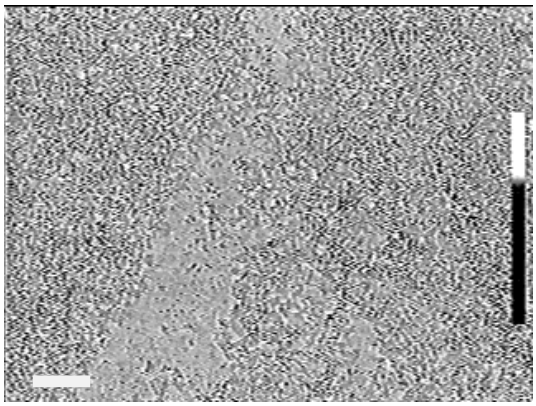

Fig. 6. A typical crack pattern for a stearic acid monolayer in the absence of 1.0 mM $CoCl_2$ and at pH 7.5. Note that no definite crack lines are seen. The bar represents 100 μm.

anisotropic, quasi-one dimensional cracking pattern is observed. This change indicates the existence of a dynamic transition, *i.e.*, the latter occurs with a slow dynamics, and the former develops instantaneously with the surface roughening. These observations are likely to be interpreted with the scenario of fracture in fragile objects such as brittle materials. Probably, the changes of viscous nature and of ion binding, and the compression direction lead to the morphology transition accompanied by a slow dynamics. The fracture in floating monolayers at the air-water interface has demonstrated that it exhibits an outstanding time dependent effect. This effect seems to be specially pronounced in these systems due to their collective behavior such as monolayer buckling due to the existence of internal degrees of freedom in amphiphilic molecules. In this study we have focused attention on the macroscopic cracking behavior in floating monolayers. A major question is what underlying microscopic structural change due to metal binding and what additional effects are responsible for the instability which induces the morphology transition and its slow dynamics. At present, this question remains unresolved. A detailed study of this question will be the subject of another report.

References

1. M. Seul, D. Andelman, Science **267**, 476 (1995).
2. O.G. Mouritsen, Int. J. Mod. Phys. B **4**, 1925 (1990).
3. R.M. Weiss, H.M. McConnell, J. Phys. Chem. **90**, 4453 (1985).
4. H. Möwald, Thin Solid Films **159**, 1 (1988).
5. D.K. Schwartz, J. Ruiz-Garcia, X. Qiu, J.V. Selinger, C.M. Knobler, Physica A **204**, 606 (1994).

6. D.K. Lubensky, R.E. Goldstein, Phys. Fluids **8**, 843 (1996), and references therein.
7. C.M. Knobler, Science **249**, 870 (1990).
8. J. Berréhar, C. Lapersonne-Meyer, M. Schott, J. Villain, J. Phys. France **50**, 923 (1989).
9. C. Allain, L. Limat, Phys. Rev. Lett. **74**, 2981 (1995).
10. E. Hatta, H. Hosoi, H. Akiyama, T. Ishii, K. Mukasa, Eur. Phys. J. B **2**, 347 (1998).
11. P. Meakin, Science **252**, 226 (1991).
12. M. Yazdanian, H. Yu, G. Zografi, Langmuir **6**, 1093 (1990).
13. H. Hosoi, H. Akiyama, E. Hatta, T. Ishii, K. Mukasa, Jpn. J. Appl. Phys. **36**, 6927 (1997).
14. H.E. Ries, Nature **281**, 287 (1979).
15. D. Bonn, H. Kellay, M. Prochnow, K. Ben-Djemiaa, J. Meunier, Science **280**, 265 (1998).
16. L.B. Freund, *Dynamical Fracture Mechanics* (Cambridge University Press, New York, 1990).
17. J.F. Boudet, S. Ciliberto, V. Steinberg, Europhys. Lett. **30**, 337 (1995).
18. R.D. Neuman, J. Colloid interface Sci. **56**, 505 (1976).
19. C. Vogel, J. Corset, M. Dupeyrat, J. Chim. Phys. **76**, 909 (1979).